Contents lists available at ScienceDirect

Arabian Journal of Chemistry

journal homepage: www.ksu.edu.sa

Original article

Design, synthesis and antibacterial activity of coumarin-3-carboxylic acid derivatives containing acylhydrazone moiety

Juncheng Liang [a,b], Xin Fu [a,c], Jing Zhang [b], Haixin Ding [d], Zhiyuan Xu [b], Huochun Ye [b], Fadi Zhu [b], Chao Yan [b], Xiuhai Gan [a,*], Gang Feng [b,*]

[a] National Key Laboratory of Green Pesticide, Key Laboratory of Green Pesticide and Agricultural Bioengineering, Ministry of Education, Center for R&D of Fine Chemicals of Guizhou University, Guiyang 550025, China
[b] Environment and Plant Protection Institute, Chinese Academy of Tropical Agricultural Science, Haikou 571101, China
[c] College of Agriculture, Heilongjiang Bayi Agricultural University, Key Laboratory of Low-carbon Green Agriculture in Northeastern China of Ministry of Agriculture and Rural Affairs, Daqing 163319, China
[d] Institute of Organic Chemistry, Jiangxi Science & Technology Normal University, Key Laboratory of Organic Chemistry, Nanchang 330013, China

ARTICLE INFO

Keywords:
Acylhydrazone
Antibacterial activity
Coumarin-3-carboxylic acid
Ralstonia solanacearum
Single-sulfoxide

ABSTRACT

Plant diseases caused by bacteria lead to enormous yield and economic losses in agricultural production. To develop innovative bactericides for controlling plant disease, a series of coumarin-3-carboxylic acid derivatives containing acylhydrazone thioether/sulfoxide were designed and synthesized by utilizing the principles of bioisosterism and active splicing. The bactericidal activities of these derivatives were subsequently evaluated. The result indicated that E2 exhibited the highest antibacterial activities *in vitro* against *Xanthomonas oryzae* pv. *oryzae*, *Ralstonia solanacearum*, and *Acidovorax citrulli*, with EC_{50} values of 2.97, 1.17, and 1.23 μg/mL, respectively. Moreover, *in vivo* experiments showed that E2 exhibited robust protective properties against *Ralstonia solanacearum*, and *Acidovorax citrulli*, with efficacies of 72.52 % and 63.90 %, respectively, at a concentration of 100 μg/mL, which was comparable to the positive control kasugamycin at the same concentration. Scanning electron microscopy analysis revealed that E2 induced changes in the cellular morphology of *Acidovorax citrulli*, such as shrinkage and collapse. Subsequent investigation revealed that E2 had the capacity to compromise the structural stability of the bacterial membrane of *Ralstonia solanacearum*. This study represents the first report on the antibacterial activities of this series of coumarin-3-carboxylic acid derivatives containing the acylhydrazone thioether/single-sulfoxide moiety, and the results suggest that coumarin-3-carboxylic acid derivatives containing the acylhydrazone single-sulfoxide may hold potential as effective antibacterial agents. And coumarin-3-carboxylic acid derivatives exhibited promise as plant bacterial agent to prevent rice bacterial leaf blight, tomato bacterial wilt, and melon bacterial fruit blotch.

1. Introduction

Plant bacterial diseases, including rice bacterial leaf blight, tomato bacterial wilt, and melon bacterial fruit blotch, caused by *Xanthomonas oryzae* pv. *oryzae* (*Xoo*), *Ralstonia solanacearum* (*Rs*) and *Acidovorax citrulli* (*Ac*), respectively, have the potential to cause a substantial reduction in crop yield and quality, thereby significantly impacting food production and security (Huang et al., 1997). For example, bacterial fruit blotch caused by *Ac* has severely cut production in Cucumis (Zhu et al., 2023). To date, the use of copper compounds and antibiotics remains a crucial method for controlling plant bacterial diseases. However, the overuse of conventional bactericides may result in the emergence of resistance to targeted pathogens, environmental contamination, and health complications (Zhang et al., 2019; Carpane et al., 2020; Chita et al., 2020). Thus, there is an immediate need to explore innovative bactericides that possess novel mechanisms of action and

Abbreviations: (^{1}H NMR), ^{1}H nuclear magnetic resonance; (^{13}C NMR), ^{13}C nuclear magnetic resonance; (HRMS), High-resolution mass spectrometry; (EC_{50}), Median effective concentration; (3-CCA), Coumarin-3-carboxylic acid; (SEM), Scanning electron microscopy; (DMSO), Dimethylsulfoxide; (*Xoo*), *Xanthomonas oryzae pv.oryzae*; *(Rs)*, *Ralstonia solanacearum*; *(Ac)*, *Acidovorax citrulli*.

Peer review under responsibility of King Saud University.

* Corresponding authors.
E-mail addresses: gxh200719@163.com (X. Gan), feng8513@sina.com (G. Feng).

https://doi.org/10.1016/j.arabjc.2023.105389
Received 28 June 2023; Accepted 24 October 2023
Available online 26 October 2023

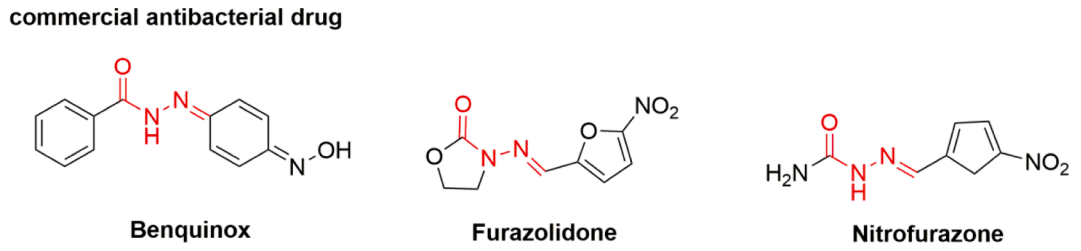

Fig. 1. The commercial antibacterial drugs containing acylhydrazone moiety.

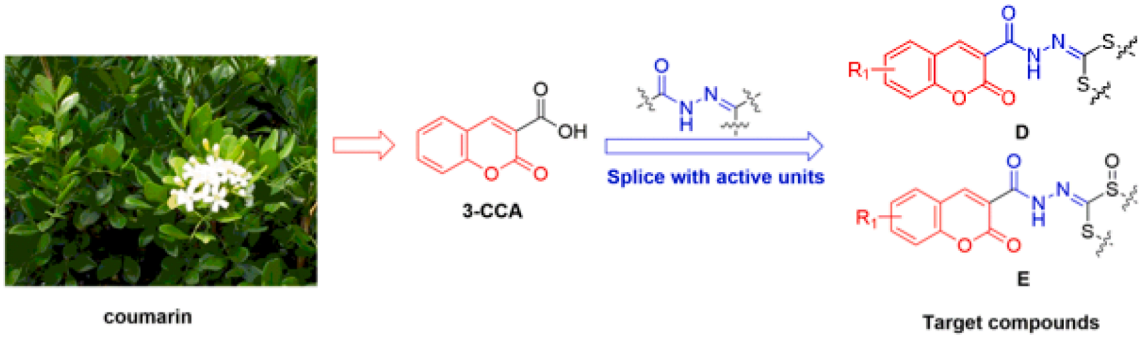

Fig. 2. Design of the target compounds.

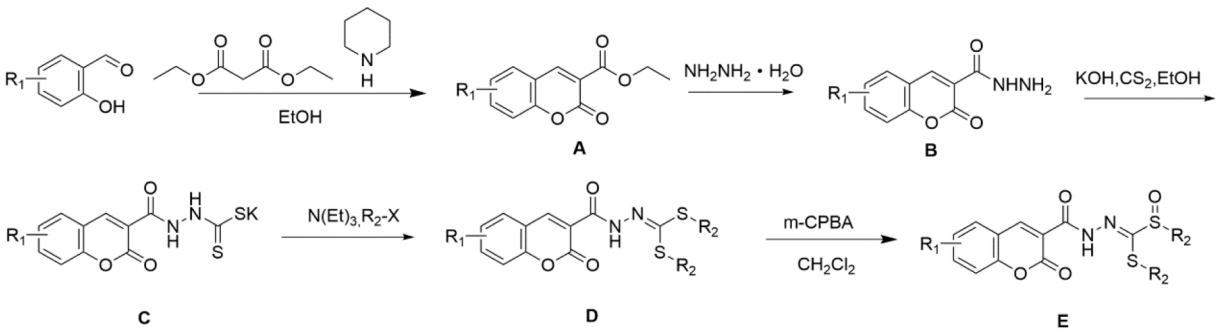

D1:R_1=H, R_2=Methyl
D2:R_1=H, R_2=Ethyl
D3:R_1=H, R_2=Propyl
D4:R_1=H, R_2=Isopropyl
D5:R_1=H, R_2=2-CH_3-benzyl
D6:R_1=7-OCH_3, R_2=Ethyl
D7:R_1=7-OCH_3, R_2=Isopropy
D8:R_1=6-F, R_2=Ethyl
D9:R_1=6-F, R_2=Propyl
D10:R_1=6-F, R_2=Isopropyl
D11:R_1=6-Cl, R_2=Ethyl
D12:R_1=6-F, R_2=Propyl

E1:R_1=H, R_2=Methyl
E2:R_1=H, R_2=Ethyl
E3:R_1=H, R_2=Propyl
E4:R_1=H, R_2=Isopropyl
E5:R_1=H, R_2=2-CH_3-benzyl
E6:R_1=7-OCH_3, R_2=Ethyl
E7:R_1=7-OCH_3, R_2=Propyl
E8:R_1=7-OCH_3R_2=Isopropyl
E9:R_1=6-F, R_2=Ethyl
E10:R_1=6-F, R_2=Propyl
E11:R_1=6-F, R_2=Isopropyl
E12:R_1=6-Cl, R_2=Ethyl
E13:R_1=6-F, R_2=Propyl

Fig. 3. Synthesis route of the target compounds.

superior efficacy in managing bacterial infections in plants.

Due to their diverse structural characteristics, unique mode of actions, and potential environmental benefits, natural products serve as a significant source of lead compounds for the development of new pesticides (Gao et al., 2007; Lin et al., 2012; Zhang et al., 2012; G et al., 2013; Gerwick and Sparks, 2014; Xiao et al., 2014; Zhang et al., 2015). Among these compounds, coumarin-3-carboxylic acid (3-CCA) has garnered considerable attention due to its multifaceted biological activities, including antitumor (Chimenti et al., 2004; Zhang et al., 2018), anticancer (Ji et al., 2020), and antimicrobial properties (Lin et al., 2012). Notably, the splicing of pyrazole amide and hydrazide at the 3-carboxyl site of 3-CCA has yielded lead compounds with enhanced antibacterial, antifungal, and anti-cancer activities, as evidenced by previous studies (Wei et al., 2017; Liu et al., 2018; Yu et al., 2018; Esfahani et al., 2021). Despite the absence of any documented reports on the antibacterial activity of 3-CCA against phytopathogenic bacteria, our previous study has revealed its remarkable broad-spectrum antibacterial properties against a diverse range of plant pathogenic bacteria and could break cell membranes (Zhu et al., 2023). Additionally, the simple structure of 3-CCA presents a promising avenue for further modification aimed at enhancing its antibacterial efficacy.

Acylhydrazone is a compound of the Schiff base variety that arises

Fig. 4. Images of the devices used in this study.

from the condensation of acylhydrazine with aldehydes or ketones. The presence of acylhydrazone in compounds confers a diverse range of biological activities, including herbicidal (Zeng et al., 2022), insecticidal (Sun et al., 2015; Ren et al., 2021), bactericidal (Abdelrahman et al., 2017; Zhang et al., 2020; Zhou et al., 2021), and antiviral properties (Chen et al., 2016; Xie et al., 2020), which are crucial in the development of novel pesticides and medicines. Notable commercial drugs that contain the acylhydrazone structure include benquinox, furazolidone, and nitrofurazone (Fig. 1). Consequently, the incorporation of acylhydrazone fragments in the development of coumarin-3-carboxylic acid derivatives with potent bactericidal activity is a viable approach.

Unfortunately, there is a lack of reported information regarding the antibacterial properties of 3-CCA derivatives that contain the acylhydrazone skeleton. As a result, this study aimed to address this gap by designing and synthesizing a range of 3-CCA derivatives that incorporated the acylhydrazone moiety (as depicted in Fig. 2 and Fig. 3) through an active splicing method. The synthesized compounds were then evaluated for their bactericidal activities, with the ultimate goal of identifying potential lead compounds for the development of innovative bactericides that can control plant diseases.

2. Materials and methods

2.1. Instruments

All chemical reagents utilized in this study were commercially available and were not subjected to further purification. The chemical reaction processes were monitored through thin-layer chromatography (TLC) under an ultraviolet lamp. The melting points of the compounds were determined using a melting point apparatus (Shanghai INESA Optical Instrument Co., Ltd., China) without temperature calibration. The ^{1}H and ^{13}C NMR spectra were obtained using a Bruker DKX500 NMR spectrometer (Bruker; Karlsruhe, Germany) with $CDCl_3$ or DMSO-d_6 as the solvent and TMS as the internal standard. The Thermo Scientific Q Exactive (Thermo Scientific, Missouri, MO) was utilized to obtain high-resolution mass spectrometry (HRMS) data of the compounds(Fig. 4).

2.2. Chemicals

The present study procured various reaction materials from Shanghai Titan Technology Co., Ltd (Shanghai, China) and other chemical materials from Bositai Technology Co., Ltd (Chongqing, China). Coumarin-3-carboxylic acid (3-CCA, 95 %) was obtained from Bide Pharmatech Ltd. (Shanghai, China), while kasugamycin (65 %) and a water solution (2 %) were sourced from Shenzhen Novoxin Agrochemical Co., Ltd (Shenzhen, China). All chemical reagents and solvents utilized in the study were of analytical purity.

2.3. Bacteria

In this study, three phytopathogenic bacterial strains, namely *Xoo* (bacterial leaf blight of rice), *Ac* (bacterial fruit blotch), and *Rs* (tomato bacterial wilt), were subjected to *in vitro* antibacterial screening. These strains were preserved for long-term use by storing them in 20 % glycerol at −80 °C. The strains were cultured either on Luria-Bertani agar (LA) plates, which contained 10 g of tryptone, 5 g of yeast extract, 10 g of NaCl, 16 g of agar, and 1 L of distilled water, or in LB broth (without agar) at 28 °C in the dark.

2.4. Synthesis

2.4.1. Synthesis of intermediates *A-C*

As shown in Fig. 3, to the solution of substituted salicylaldehyde (10 mmol) in EtOH was added, diethyl malonate (12 mmol) and piperidine (2 mmol) under an argon atmosphere. After addition, the reaction mixture was heated to reflux for 12 h to produce intermediates **A**. Then using dichloromethane as the solvent, intermediates **A** (10 mmol) and hydrazine hydrate (15 mmol) were stirred at −5°C for 10–30 mins. Intermediates **B** were saturated with sodium chloride and extracted with dichloromethane. Subsequently, the intermediates **B**, KOH (12 mmol), and carbon disulphide (15 mmol) were mixed and refluxed in ethanol. After the completion of the reaction as monitored by TLC, the solvent was removed in vacuum. The raw product was washed with ethanol to obtain intermediates **C**.

2.4.2. Synthesis of target compounds *D1-D12*

To the solution of intermediates **C** (10 mmol) in DMF (25 mL) was added different halogenated hydrocarbons (24 mmol) and potassium carbonate (15 mmol). The reaction mixture was stirred for 5–8 h at room temperature until TLC detection showed the reaction was finished. The saturated aqueous ammonium chloride solution was poured into the reaction mixture to obtain a crude product, which was purified by recrystallization or column chromatography to get target compounds **D1**-**D12**.

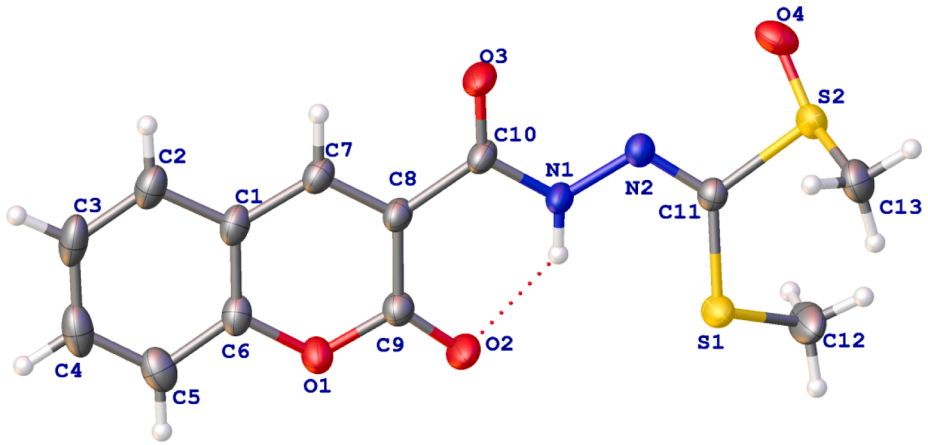

Fig. 5. X-ray crystal structure of compound **E2.**

2.4.3. Synthesis of target compounds *E1-E13*

Based on the target compounds **D**, the target compounds **E** (10 mmol) were oxidized by m-CPBA (12 mmol) with CH_2Cl_2 as the solvent at room temperature, then target compounds **E1-E13** were obtained by extraction and purification. The structures of target compounds were confirmed with ^{1}H NMR, ^{13}C NMR, and HRMS, and the data are described in the Supporting Information.

The representative data for compound **E2** are presented in the following: *ethyl (E)-(ethylsulfinyl)-N-(2-oxo-2H-chromene-3-carbonyl) methanehydrazonothioate* (**E2**): Yield: 27.93 %, yellow solid, m.p. 142.4–143.7 ℃. ^{1}H NMR (400 MHz, $CDCl_3$) δ 12.58 (s, 1H), 9.08 (s, 1H), 7.79–7.74 (m, 2H), 7.50–7.42 (m, 2H), 3.39–3.30 (m, 1H), 3.23–3.01 (m, 3H), 1.42 (t, J = 7.4 Hz, 3H), 1.35 (t, J = 7.5 Hz, 3H). ^{13}C NMR (101 MHz, $CDCl_3$) δ 161.19, 158.40, 157.63, 154.71, 150.81, 135.21, 130.27, 125.77, 118.41, 117.17, 116.90, 47.70, 28.99, 16.05, 6.89. HRMS (ESI) m/z for $C_{15}H_{16}O_4N_2NaS_2$ $[M + H]^+$ calcd: 375.04437, found: 375.04309.

2.4.4. X-ray diffraction

X-ray single-crystal diffraction experiments were conducted at a temperature of 170 K, using Cu Kα rays as the incident light. The data collection angles ranged from 8.192° to 144.272°, and the independent diffraction points were 2613 (Rint = 0.0284, Rsigma = 0.0307). Compound **E2** was recrystallized from a mixture of ethanol and dichloromethane to obtain a suitable single crystal, with dimensions of 0.14 mm × 0.12 mm × 0.1 mm for diffraction analysis.

2.5. Antibacterial activity test in vitro

In *vitro,* antimicrobial activities of all target compounds against *Xoo*, Rs and *Ac* were evaluated using a turbidity assay (Li et al., 2014), with kasugamycin and 3-CCA as the positive control and dimethyl sulfoxide (DMSO) as the blank control. The concentrations of compounds used for screening were 50 and 25 μg/mL respectively.

2.6. Antibacterial activities of E2 against Ac and Rs in vivo

In vivo, antibacterial activities of target compound E2 against *Ac* and *Rs* were evaluated by greenhouse pot experiments (Li et al., 2013; Li et al., 2015; Wang et al., 2016; Seong et al., 2019) respectively. Kasugamycin water solution (2 %) was used as the positive control. The disease symptoms were evaluated each day after inoculation using a disease index (DI) calculated from a modified 0 to 9 disease severity scale: 0, no symptoms; 1, 3, 5 and 7, necrotic lesions on approximately 25 %, 50 %, 75 % and 100 % of the cotyledons, respectively; and 9, total death of the seedling. The disease index and control effect were calculated each day based on the following formula:

$$Diseaseindex = \frac{\Sigma(Thenumberofdiseasedleavesineachgrade \times correspondinggradevalue)}{totalnumberofleavesinvestigated \times thehighestdiseasegradevalue} \times 100$$

$$Controleffect(\%) = \frac{Diseaseindexinthecontrolgroup - Diseaseindexinthetreatedgroup}{Diseaseindexinthecontrolgroup} \times 100$$

2.7. Observation of microstructure

The morphologies and microstructures of compound **E2** against *Ac* were observed by scanning electron microscopy (SEM) (Liu et al., 2021).

2.8. Effect of E2 on the membrane integrity of Rs

The present study assessed the effect of E2 on the membrane permeability of *Ac*, utilizing the methodology outlined by (Ernst et al. 2000). A suspension of Rs bacteria was prepared and subjected to varying concentrations of E2, employing the same procedures as the previous membrane permeability analysis. Following a 4-hour treatment, the bacteria were collected via centrifugation at 12000 × g for 5 min and subsequently incubated with propidium iodide (PI, 30 μM) for 20 min in the dark at room temperature. Subsequently, the unbound dye underwent a comprehensive washing process with the PBS buffer, and the PI fluorescence of both treated samples and controls was assessed via flow cytometry. The experimentation was conducted thrice, with each treatment executed in triplicate.

Table 1
Antibacterial activity of 3-CCA derivatives against *Xoo*, *Rs* and *Ac*.

Sample	Inhibition (%)					
	Xoo		*Rs*		Ac	
	50 μg/mL	25 μg/mL	50 μg/mL	25 μg/mL	50 μg/mL	25 μg/mL
D1	32.46	22.13	3.98	4.71	15.07	11.77
D2	27.15	21.54	5.41	2.74	6.41	5.75
D3	50.42	47.2	1.78	0.31	9.69	6.98
D4	19.49	9.64	15.69	13.32	14.69	8.61
D5	18.75	6.53	8.40	5.65	16.37	6.34
D6	46.93	44.57	1.58	0.25	41.82	17.42
D7	37.19	31.47	2.99	11.01	10.57	0.45
D8	31.88	24.7	0.46	0.26	14.68	8.60
D9	59.03	48.46	7.54	0.68	10.15	5.45
D10	45.11	2.21	1.16	0.26	11.58	11.50
D11	43.73	0.46	21.52	19.24	18.16	3.97
D12	4.06	4.33	13.88	6.71	32.61	26.75
E1	92.93	89.76	99.06	96.64	99.97	98.16
E2	96.21	93.17	95.94	94.54	99.75	94.16
E3	93.83	87.09	99.99	99.91	74.86	54.40
E4	41.38	38.84	13.55	7.61	12.33	5.84
E5	46.47	39.40	14.23	11.88	7.91	2.23
E6	82.91	63.11	88.15	60.10	68.25	47.49
E7	95.87	93.69	99.23	79.06	97.80	98.23
E8	88.05	84.69	97.17	88.75	98.55	97.44
E9	71.82	62.10	74.97	58.95	70.61	42.46
E10	7.45	0.33	19.13	12.38	30.72	28.77
E11	86.48	69.87	97.84	39.19	25.76	5.72
E12	92.69	80.81	56.34	5.87	55.28	28.06
E13	80.61	32.56	6.84	5.48	70.79	57.72
3-CCA	47.68	38.18	61.40	47.52	57.23	38.95
Kasugamycin	91.92	90.83	98.94	86.55	98.59	32.36

2.9. Statistical analyses

The SPSS software (version 20.0, IBM Corp., Armonk, NY, USA) was utilized for variance analysis during data analysis. Statistical significance was determined as $P < 0.05$ through the application of Duncan's Multiple Range Test, and the outcomes were depicted in lowercase alphabets in both figures and tables. Sigma Plot (version 12.5, Systat Software Inc., San Jose, CA, USA) was employed to generate graphs.

3. Results and discussion

3.1. Chemistry

The synthesis of target compounds is illustrated in Fig. 3, and synthetic procedures and methods are described in the Materials and Methods section. The structures of the target compounds were confirmed through the analysis of ^{1}H NMR, ^{13}C NMR and HRMS data, which were listed in the Supporting Information. Furthermore, the structure of compound E2 was authenticated via X-ray diffraction analysis, as depicted in Fig. 5.

3.2. Antibacterial activity of 3-CCA derivatives against Xoo, Rs and Ac in vivo

The *in vitro* antibacterial activity of twenty-five 3-CCA derivatives containing acylhydrazone thioether and single-sulfoxide moieties were determined against *Xoo*, *Rs* and *Ac*. The results were tabulated in Table 1. Notably, the acylzone-sulfoxide compounds **E1** and **E2** exhibited significant efficacy in controlling plant pathogenic bacteria at a concentration of 50 μg/mL, with inhibitions of 96.21 %, 95.94 % and 99.75 % against *Xoo*, *Rs* and *Ac*, respectively. These values were higher than those of the lead compound 3-CCA and were comparable to the positive control kasugamycin. Compound **E3**, an acylzone-sulfoxide, exhibited significant antibacterial activity against *Xoo* and *Rs*, with inhibitory rates of 93.83 % and 99.99 % at a concentration of 50 μg/mL,

Table 2
EC_{50} values of high-activity compounds against *Xoo*, *Rs* and *Ac*.

Bacteria	Compounds	LC-P	r	EC_{50} (μg/mL)	95 %FL (μg/mL)
Xoo	**E1**	Y = 3.9752 + 1.9151x	0.9653	3.43	2.35–5.00
	E2	Y = 4.3844 + 1.3012x	0.9743	2.97	1.95–4.52
	E3	Y = 4.0204 + 1.5017x	0.9839	4.49	3.11–6.48
	E6	Y = 3.7316 + 1.3528x	0.9983	8.66	5.96–12.58
	E7	Y = 4.2631 + 1.5348x	0.9929	3.02	2.00–4.56
	E8	Y = -3.8780 + 1.9498x	0.9980	3.76	2.77–5.12
	3-CCA	Y = 2.6739 + 1.5292x	0.9952	33.20	22.97–47.99
	Kasugamycin	Y = 4.1624 + 1.1718x	0.9464	5.19	3.30–8.15
Rs	**E1**	Y = 4.4807 + 1.8019x	0.9813	1.94	1.43–2.64
	E2	Y = 4.9010 + 1.4810x	0.9507	1.17	0.77–1.78
	E3	Y = 4.0498 + 1.4119x	0.9815	4.71	3.21–6.92
	E6	Y = 4.0023 + 1.0729x	0.9968	8.51	5.05–14.34
	E7	Y = 4.3511 + 1.4173x	0.9610	2.87	1.95–4.23
	E8	Y = 4.3441 + 1.4788x	0.9690	2.78	1.91–4.03
	3-CCA	Y = 3.3851 + 1.1059x	0.9960	28.86	18.16–45.85
	Kasugamycin	Y = 3.9657 + 1.3179x	0.9940	6.09	4.04–9.19
Ac	**E1**	Y = 4.4881 + 1.3112x	0.9895	2.46	1.63–3.69
	E2	Y = 4.8650 + 1.5056x	0.9965	1.23	0.82–1.85
	E3	Y = 4.0763 + 1.0702x	0.9831	7.30	4.44–12.00
	E6	Y = 4.0282 + 0.9750x	0.9998	9.92	5.53–17.80
	E7	Y = 4.1132 + 1.7174x	0.9941	3.28	2.29–4.71
	E8	Y = 4.0509 + 1.5035x	0.9691	4.28	2.97–6.17
	3-CCA	Y = 3.3787 + 1.1849x	0.9932	23.35	15.24–35.79
	Kasugamycin	Y = 3.9056 + 1.1019x	0.9852	9.85	5.81–16.67

respectively. These rates were higher than those of the lead compounds and comparable to the positive control. Conversely, the bactericidal activity of acylhydrazone thioethers was observed to be lower, ranging from 4 % to 47 %.

The antibacterial activity of compounds **E6**-**E8**, which were modified with 7-methoxyl, was found to be higher than that of acylhydrazone thioether but lower than that of E1-E3. At a concentration of 50 μg/mL, these compounds were effective against *Xoo*, *Rs*, and *Ac*, with inhibition rates ranging from 60.10 % to 98.55 %. Additionally, compounds **E9**, **E11**, **E12**, and **E13**, which were derived from 6-chloro and 6-fluoro, exhibited strong selective antibacterial activity against *Xoo*, with inhibition rates of 71.82 %, 86.48 %, 92.69 %, and 80.61 % at 50 μg/mL, respectively.

The aforementioned results suggested that the 3-carboxyl moiety might serve as the active site of 3-CCA, thereby presenting a promising avenue for further modifications aimed at developing more potent antibacterial agents. To this end, a total of twenty-five 3-CCA derivatives were synthesized in this investigation through the incorporation of acylhydrazone thioether and single-sulfoxide groups at the 3-carboxyl position of the parent compound. The results obtained indicate that

Table 3
The protective and curative effect of **E2** against *Ac in vivo*.

Sample	Concentration (μg/mL)	Protective effect		Curative effect	
		Disease index	efficacy (%)	Disease index	efficacy (%)
E2	25	38.68 ± 3.56b	35.24c	53.91 ± 1.89b	25.90c
	50	23.46 ± 2.14c	60.70b	35.80 ± 1.23c	50.83b
	100	16.46 ± 2.57d	72.52a	27.16 ± 2.14d	62.63a
Kasugamycin	100	16.87 ± 2.85d	71.84a	26.60 ± 2.76d	63.40a
control	/	59.67 ± 3.77a	/	72.84 ± 2.47a	/

Note: Columns represent the mean ± SE. Different letters in the column represent significant difference at $P_{0.05}$ level, the same as following.

the antibacterial activities of 3-CCA derivatives containing acylhydrazone single-sulfoxide outperformed those containing acylhydrazone thioether. Furthermore, the bacterial activity was significantly impacted by the substituent R2. The structure–activity relationship (SAR) analysis of R2 substitutions revealed that the substitution of R2 with benzyl or bulky groups resulted in reduced antibacterial activity compared to methyl or ethyl groups, which was consistent with the findings of (Zhang et al. 2022). Nevertheless, the structural modifications had an overall detrimental effect on the activity, and no beneficial substitution for the benzene ring of coumarin was observed. The introduction of F and Cl as electron withdrawing groups resulted in a significant reduction in antibacterial activity compared to the absence of substituents. Similarly, the introduction of a methoxy group as an electron donor group resulted in inferior antibacterial activity. Consequently, the sulfoxide moiety may serve as an antibacterial fragment, and sulfoxide compounds may have the potential as antibacterial agents against plant diseases.

3.3. Bacterial virulence assays of high activity compounds

Based on the results of the initial screening, high-activity compounds, namely compounds **E1**, **E2**, **E3**, **E6**, **E7** and **E8**, were selected for further investigation of their antibacterial virulence. As presented in Table 2, E2 exhibited the most potent antibacterial activity against *Xoo*, *Rs* and *Ac*, with EC_{50} values of 2.97 μg/mL, 1.17 μg/mL and 1.23 μg/mL, respectively, surpassing those of the lead compound 3-CCA and the positive control kasugamycin. Similarly, E1 also demonstrated remarkable bactericidal activity against *Xoo*, *Rs* and *Ac*, with EC_{50} values of 3.43 μg/mL, 1.94 μg/mL and 2.46 μg/mL, respectively. However, other modification sites of coumarins also showed moderate antibacterial activity which EC_{50} values ranged from 2.78 to 9.92 μg/mL on Xoo, Rs and *Ac* respectively.

3.4. Bacterial activity of E2 against Ac and Rs in vivo

Pot experiments were undertaken to investigate the protective and curative properties of **E2** against *Ac* (Table 3 and Fig. 6). The results indicated that **E2** demonstrated a remarkable protective effect against

Table 4
The protective and curative effect of **E2** against *Rs in vivo*.

Sample	Concentration (μg/mL)	Protective effect		Curative effect	
		Disease index	efficacy (%)	Disease index	efficacy (%)
E2	25	30.04 ± 1.43b	44.45c	43.89 ± 6.01b	33.08d
	50	23.87 ± 2.85c	56.11b	34.57 ± 3.27c	47.15c
	100	19.75 ± 4.28d	63.90a	29.01 ± 1.85d	55.55b
Kasugamycin	100	19.34 ± 1.43d	64.34a	25.93 ± 2.14d	60.34a
control	/	54.32 ± 5.38a	/	65.43 ± 6.42a	/

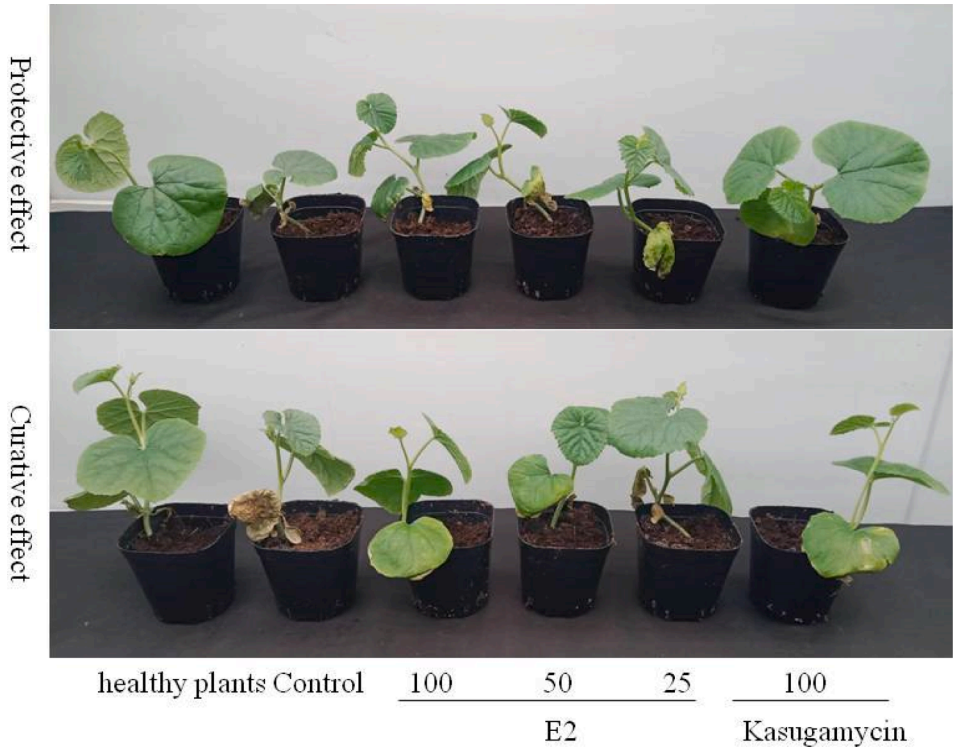

Fig. 6. The protective and curative effect of **E2** against melon bacterial fruit blotch *in vivo*.

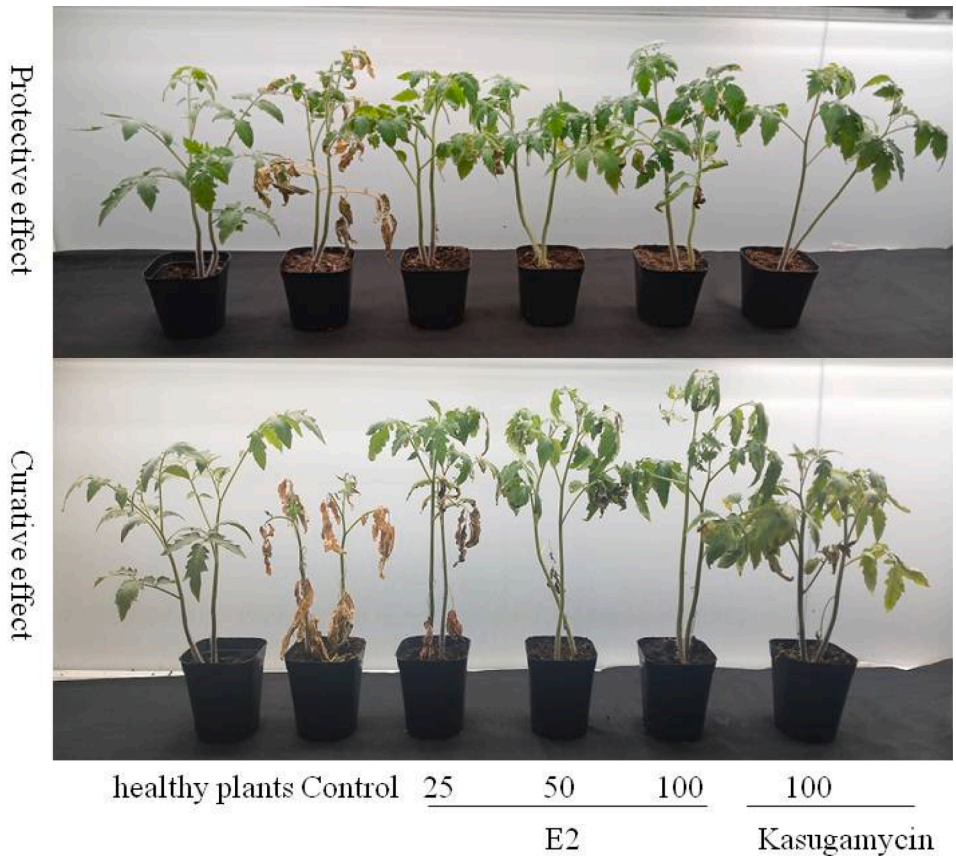

Fig. 7. The protective and curative effect of **E2** against tomato bacterial wilt *in vivo*.

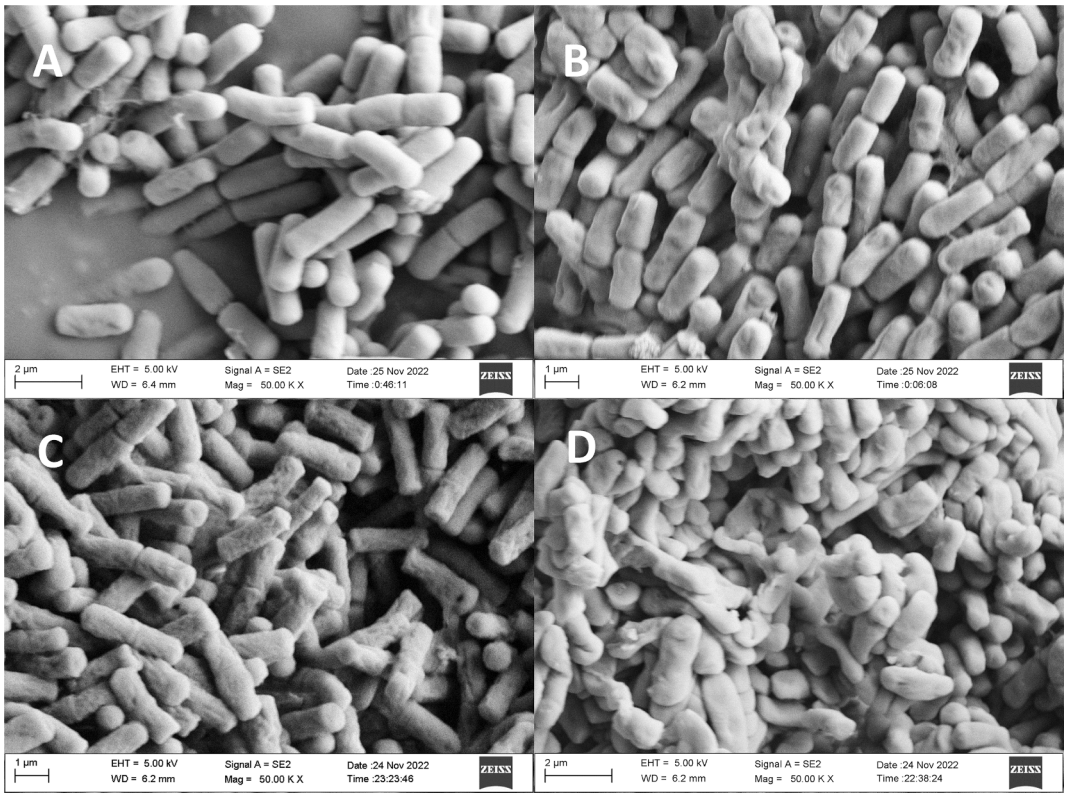

Fig. 8. SEM observations of *Rs* treated with **E2** (A) CK; (B) **E2** at 1.25 μg/ mL; (C) **E2** at 2.5 μg/ mL and (D) **E2** at 5 μg/ mL.

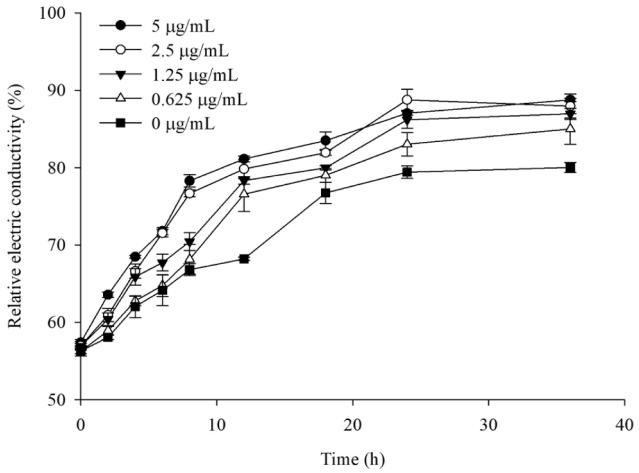

Fig. 9. Effect of compound **E2** on relative conductivity of *Rs*.

Ac, with an efficacy of 72.52 % at a concentration of 100 μg/mL. This efficacy was comparable to that of the positive control, kasugamycin (71.84 %), and significantly superior to other concentrations. Furthermore, **E2** exhibited significant curative effects against *Ac*, with a curative efficacy of 62.07 % at the same concentration. No significant difference was observed when compared to the control agent, kasugamycin (63.40 %).

The results of our study indicated that **E2** exhibited remarkable protective and curative effects against *Rs in vivo*, as evidenced by the data presented in Table 4 and Fig. 7. Specifically, the efficacy of **E2** against *Rs* was determined to be 63.90 % at a concentration of 100 μg/mL, which was not significantly different from that of Kasugamycin (64.34 %). Additionally, E2 demonstrated a moderate curative effect against Rs, with an efficacy of 55.55 % at 100 μg/mL, which was lower than that of kasugamycin (60.34 %).

3.5. *Effect of **E2** on the hyphae morphology of Rs*

The present study utilized scanning electron microscopy to investigate the effect of **E2** on the ultrastructure of *Rs*. The results, depicted in Fig. 8, indicate that the control treatment (7-A) yielded bacterial cells that were characterized by a mellow, full, elongated, and rod-shaped morphology. However, exposure to 1.25 μg/mL of **E2** resulted in some cells displaying depression (7-B), and as the concentration of **E2** increased, the cells exhibited more severe shrinkage (7-C). Notably, cells treated with 5 μg/mL of **E2** displayed significant shrinkage and distortion (7-D).

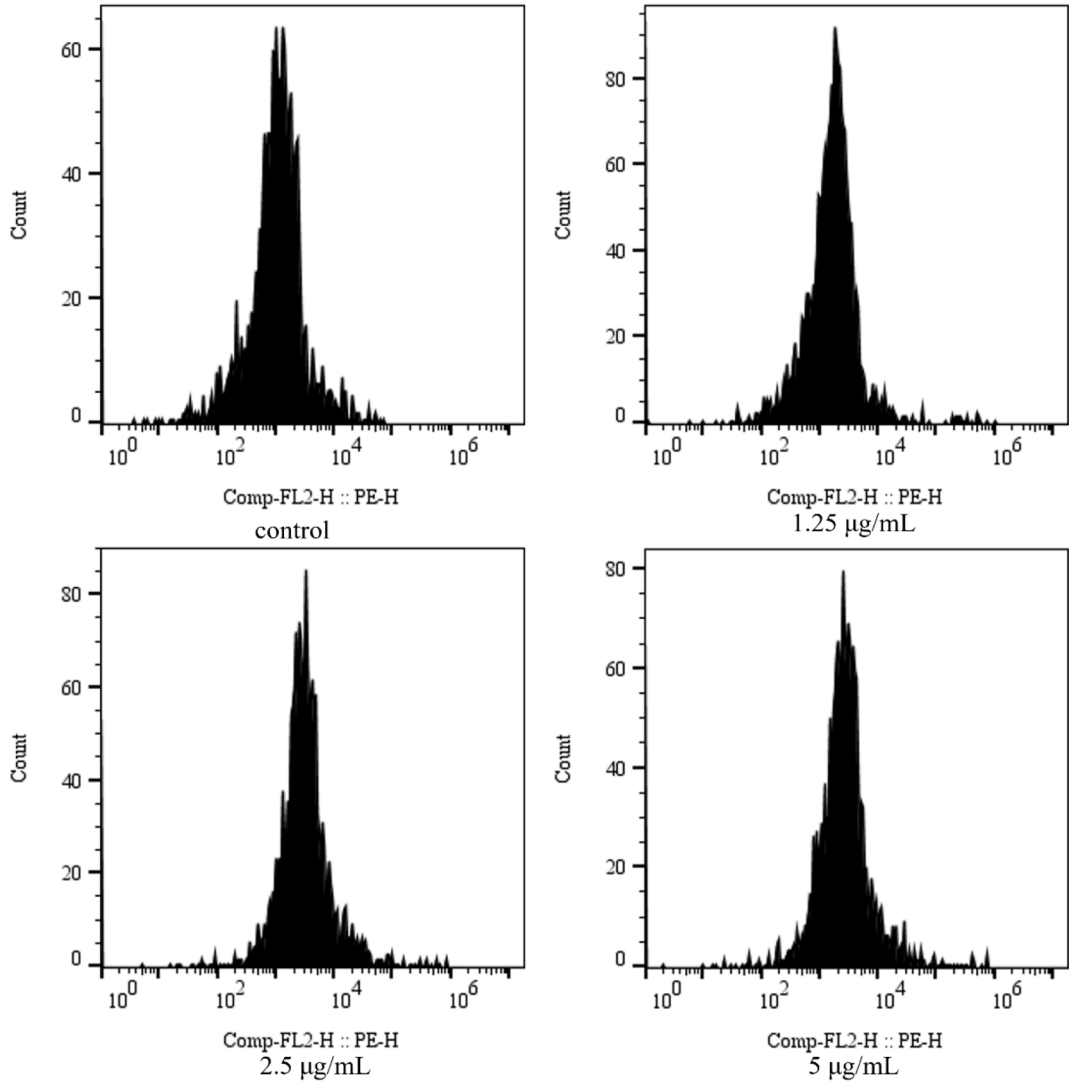

Fig. 10. Effect of compound **E2** on cell membrane integrity of *Rs*.

3.6. Effects of E2 on cell membrane integrity of Rs

This study employed a conductivity meter and flow cytometer to assess the impact of **E2** on the integrity of the *Rs* cell membrane. The findings indicated that the relative conductivity of the solution increased when the bacterial cell membrane was compromised releasing of intracellular electrolytes. By measuring the relative electrical conductivity, the effect of **E2** on cell membrane permeability could be determined. The findings, illustrated in Fig. 9, indicated a direct correlation between the concentrations of **E2** and the conductivity values. Notably, a marked escalation in relative conductivity was observed at the 4-hour mark post-treatment, with the conductivity values of **E2** at 1.25, 2.5 and 5 μg/mL significantly surpassing those of the control. The conductivity values for all treatments reached their zenith at the 24-hour mark post-treatment.

The bacterial cell membrane can be penetrated by PI, which subsequently binds to nucleic acid and elicits a fluorescence response that can be detected via flow cytometry. This fluorescence response is frequently employed to evaluate the integrity of the bacterial cell membrane. As illustrated in Fig. 10, the fluorescence intensity was primarily distributed between 0 and 10^5 in the absence of **E2** treatment. However, following **E2** treatment, the fluorescence intensity of *Rs* increased. Furthermore, the fluorescence intensity increased progressively with increasing **E2** concentrations, peaking at a concentration of 5 μg/mL.

The cell membrane is a critical component in maintaining the structural integrity of cells and facilitating normal cellular functions, rendering it a crucial target for antibacterial interventions (Hendrich et al., 2003). Several natural antibacterial agents, including thymol (Harnvoravongchai et al., 2018), protocatechualdehyde (Li et al., 2016), and berberine (Peng et al., 2015), can exert antibacterial effects by modifying the permeability and integrity of bacterial cell membranes (Ismail et al., 2020; Langeveld et al., 2014). The findings of this study demonstrated that treatment of *Rs* cells with **E2** resulted in a characteristic wrinkled and withered surface, increased conductivity, and elevated fluorescence intensity of PI bound to the nucleus. These results indicated **E2** could significantly undermine the integrity of the *Rs* cell membrane.

4. Conclusions

In summary, a total of twenty-five novel 3-CCA derivatives containing the acylhydrazone were synthesized, and several compounds demonstrated noteworthy antibacterial properties. Notably, compound E2 exhibited the most potent antibacterial activities against *Rs* and *Ac* both *in vitro* and *in vivo*, and disrupted bacterial membrane integrity, resulting in significant antimicrobial activity. The findings from the analysis of structural-activity relationship indicated that 3-CCA derivatives containing an acylhydrazone single-sulfoxide moiety with short linear alkane substituents (methyl/ethyl) exhibited a significantly higher antibacterial activity compared to those substituted with benzyl or other large groups. This study represents the first report on the antibacterial activities of this particular series of 3-CCA derivatives containing the acylhydrazone thioether/single-sulfoxide moiety, and the results suggest that 3-CCA derivatives containing the acylhydrazone single-sulfoxide may hold potential as effective antibacterial agents. And coumarin-3-carboxylic acid derivatives exhibited promise as plant bacterial agent to prevent rice bacterial leaf blight, tomato bacterial wilt, and melon bacterial fruit blotch.

Declaration of Competing Interest

The authors declare that they have no known competing financial interests or personal relationships that could have appeared to influence the work reported in this paper.

Acknowledgement

This work was supported financially by the High-level Talents Foundation of Basic and Applied Basic Research Plan (Natural Science Field) of Hainan Province(320RC697), Key Laboratory of Low-carbon Green Agriculture in Northeastern China, Ministry of Agriculture and Rural Affairs P. R. China (Grant No.LCGANE08), the National Natural Science Foundation of China (NSFC No. 32372598), the Fundamental Research Fund of Academy of Tropical Agricultural Science (1630042022009) and Chinese Academy of Tropical Agricultural Sciences for Science and Technology Innovation Team of National Tropical Agricultural Science Center (CATASCXTD202305).

Appendix A. Supplementary material

Characterization data, ^{1}H and ^{13}C NMR spectra and HRMS of compounds **D1-D12**, and **E1-E13** are described in the Supporting Information. Supplementary data to this article can be found online at https://doi.org/10.1016/j.arabjc.2023.105389.

References

Abdelrahman, M.A., Salama, I., Gomaa, M.S., Elaasser, M.M., Abdel-Aziz, M.M., Soliman, D.H., 2017. Design, synthesis and 2D QSAR study of novel pyridine and quinolone hydrazone derivatives as potential antimicrobial and antitubercular agents. Eur. J. Med. Chem. 138, 698–714.

Carpane, P.D., Peper, A.M., Kohn, F., 2020. Management of northern corn leaf blight using nativo (trifloxistrobin + tebuconazole) fungicide applications. Crop Prot. 127, 104982.

Chen, L.W., Xie, J.L., Song, H.J., Liu, Y.X., Gu, Y.C., Wang, L.Z., Wang, Q.M., 2016. Design, synthesis, and biological activities of spirooxindoles containing acylhydrazone fragment derivatives based on the biosynthesis of alkaloids derived from tryptophan. J. Agric. Food Chem. 64, 6508–6516.

Chimenti, F., Secci, D., Bolasco, A., Chimenti, P., Granese, A., Befani, O., Turini, P., Alcaro, S., Ortuso, F., 2004. Inhibition of monoamine oxidases by coumarin-3-acyl derivatives: biological activity and computational study. Bioorg. Med. Chem. Lett. 14, 3697–3703.

Ernst, W.A., Thoma-Uszynski, S., Teitelbaum, R., Ko, C., Hanson, D.A., Clayberger, C., Krensky, A.M., Leippe, M., Bloom, B.R., Ganz, T., Modlin, R.L., 2000. Granulysin, a T cell product, kills bacteria by altering membrane permeability. J. Immunol. 165, 7102–7108.

Esfahani, S.N., Damavandi, M.S., Sadeghi, P., Nazifi, Z., Salari-Jazi, A., Massah, A.R., 2021. Synthesis of some novel coumarin isoxazol sulfonamide hybrid compounds, 3D-QSAR studies, and antibacterial evaluation. Sci. Rep. 11, 20088.

Gao, J.M., Wu, W.J., Zhang, J.W., Konishi, Y., 2007. The dihydro-β-agarofuran sesquiterpenoids. Nat. Prod. Rep. 24, 1153–1189.

Gerwick, B.C., Sparks, T.C., 2014. Natural products for pest control: An analysis of their role, value and future. Pest Manage. Sci. 70, 1169–1185.

Harnvoravongchai, P., Chankhamhaengdecha, S., Ounjai, P., Singhakaew, S., Boonthaworn, K., Janvilisr, T., 2018. Antimicrobial effect of asiatic acid against *Clostridium difficile* is associated with disruption of membrane permeability. Front. Microbiol. 9, 2125.

Hendrich, A.B., Michalak, K., 2003. Lipids as a target for drugs modulating multidrug resistance of cancer cells. Curr. Drug Targets 4, 23–30.

Huang, N., Angeles, E.R., Domingo, J., Magpantay, G., Singh, S., Zhang, G., Kumaravadivel, N., Bennett, J., Khush, G.S., 1997. Pyramiding of bacterial blight resistance genes in rice: Markerassisted selection using RFLP and PCR. Theor. Appl. Genet. 95, 313–320.

Ismail, W., Ezzat, S., Michel, H., Deeb, K.E., Fishawy, A.E., 2020. Angiotensin-converting enzyme and renin inhibition activities, antioxidant properties, phenolic and flavonoid contents of *Cuphea ignea* A. DC. J. Reports Pharm. Sci. 9, 92–96.

Ji, H., Tan, Y.L., Gan, N.N., Zhang, J., Li, S.N., Zheng, X., Wang, Z.H., Yi, W., 2020. Synthesis and anticancer activity of new coumarin-3-carboxylic acid derivatives as potential lactate transport inhibitors. Bioorg. Med. Chem. 29, 115870.

Langeveld, W.T., Veldhuizen, E.J.A., Burt, S.A., 2014. Synergy between essential oil components and antibiotics: A review. Crit. Rev. Microbiol. 40, 76–94.

Li, G.H., Qiao, M.Y., Guo, Y., Wang, X., Xu, Y.F., Xia, X.D., 2014. Effect of subinhibitory concentrations of chlorogenic acid on reducing the virulence factor production by *Staphylococcus aureus*. Foodborne Pathog. Dis. 11, 677–683.

Li, B., Shi, Y., Shan, C.L., Zhou, Q., Ibrahim, M., Wang, Y.L., Wu, G.X., Li, H.Y., Xie, G.L., Sun, G.C., 2013. Effect of chitosan solution on the inhibition of *Acidovorax citrulli* causing bacterial fruit blotch of watermelon. J. Sci. Food Agric. 93, 1010–1015.

Li, P., Shi, L., Gao, M.N., Yang, X., Xue, W., Jin, L.H., Hu, D.Y., Song, B.A., 2015. Antibacterial activities against rice bacterial leaf blight and tomato bacterial wilt of 2-mercapto-5-substituted-1,3,4-oxadiazole/thiadiazole derivatives. Bioorg. Med. Chem. Lett. 25, 481–484.

Li, S.L., Yu, Y.M., Chen, J.N., Guo, B., Yang, L., Ding, W., 2016. Evaluation of the antibacterial effects and mechanism of action of protocatechualdehyde against *Ralstonia solanacearum*. Molecules 21, 754.

Lin, L., Mulholland, N., Wu, Q.Y., Beattie, D., Huang, S.W., Irwin, D., Clough, J., Gu, Y.C., Yang, G.F., 2012. Synthesis and antifungal activity of novel sclerotiorin analogues. J. Agric. Food Chem. 60, 4480–4491.

Lin, P.Y., Yeh, K.S., Su, C.L., Sheu, S.Y., Chen, T., Ou, K.L., Lin, M.H., Lee, L.W., 2012. Synthesis and antibacterial activities of novel 4-hydroxy-7-hydroxy- and 3-carboxycoumarin derivatives. Molecules 17, 10846–10863.

Liu, H., Ren, Z.L., Gong, J.X., Chu, M.J., Ma, Q.W., Wang, J.C., Lv, X.H., 2018. Novel coumarin-pyrazole carboxamide derivatives as potential topoisomerase II inhibitors: Design, synthesis, and antibacterial activity. Eur. J. Med. Chem. 157, 81–87.

Liu, T., Ren, X., Cao, G., Zhou, X., Jin, L., 2021. Transcriptome analysis on the mechanism of ethylicin inhibiting *Pseudomonas syringae* pv. *actinidiae* on kiwifruit. Microorganisms 9, 724.

Peng, L.C., Kang, S., Yin, Z.Q., Jia, R.Y., Song, X., Li, L., Li, Z.W., Zou, Y.F., Liang, X.X., Li, L.X., He, C.L., Ye, G., Yin, L.Z., Shi, F., Lv, C., Jing, B., 2015. Antibacterial activity and mechanism of berberine against *Streptococcus agalactiae*. Int. J. Clin. Exp. Path. 8, 5217–5223.

Ren, Z.L., Lv, M., Sun, Z.Q., Li, T.Z., Zhang, S.Y., Xu, H., 2021. Regioselective hemisynthesis and insecticidal activity of C8-hydrazones/acylhydrazones/sulfonylhydrazones coumarin-type derivatives of osthole. Bioorg. Med. Chem. Lett. 40, 127962.

Sun, J.L., Zhou, Y.M., 2015. Design, synthesis, and insecticidal activity of some novel diacylhydrazine and acylhydrazone derivatives. Molecules 20, 5625–5637.

Wang, T.L., Guan, W., Huang, Q., Yang, Y.W., Yan, W.R., Sun, B.X., Zhao, T.C., 2016. Quorum-sensing contributes to virulence, twitching motility, seed attachment and biofilm formation in the wild type strain Aac-5 of *Acidovorax citrulli*. Microb. Pathog. 100, 133–140.

Wei, L., Wang, J.X., Zhang, X.L., Wang, P., Zhao, Y.P., Li, J.Q., Hou, T., Qu, L.L., Shi, L.Y., Liang, X.M., Fang, Y., 2017. Discovery of 2H-chromen-2-one derivatives as G Protein-Coupled Receptor-35 agonists. J. Med. Chem. 60, 362–372.

Xiao, J., Zhang, Q., Gao, Y.Q., Tang, J.J., Zhang, A.L., Gao, J.M., 2014. Secondary metabolites from the endophytic *Botryosphaeria dothidea* of *Melia azedarach* and their antifungal, antibacterial, antioxidant, and cytotoxic activities. J. Agric. Food Chem. 62, 3584–3590.

Xie, J.L., Xu, W.T., Song, H.J., Liu, Y.X., Zhang, J.J., Wang, Q.M., 2020. Synthesis and antiviral/fungicidal/insecticidal activities study of novel chiral indole diketopiperazine derivatives containing acylhydrazone moiety. J. Agric. Food Chem. 68, 5555–5571.

Yu, X., Teng, P., Zhang, Y.L., Xu, Z.J., Zhang, M.Z., Zhang, W.H., 2018. Design, synthesis and antifungal activity evaluation of coumarin-3-carboxamide derivatives. Fitoterapia 127, 387–395.

Zeng, H.N., Zhang, W., Wang, Z.X., Geng, W., Feng, G., Gan, X.H., 2022. Novel pyrazole amides as potential 4-hydroxyphenylpyruvate dioxygenase inhibitors. J. Agric. Food Chem. 70, 7400–7411.

Zhang, Z., Bai, Z.W., Ling, Y., He, L.Q., Huang, P., Gu, H.X., Hu, R.F., 2018. Design, synthesis and biological evaluation of novel furoxan-based coumarin derivatives as antitumor agents. Med. Chem. Res. 27, 1198–1205.

Zhang, M.Z., Chen, Q., Mulholland, N., Beattie, D., Irwin, D., Gu, Y.C., Yang, G.F., Clough, J., 2012. Synthesis and fungicidal activity of novel pimprinine analogues. Eur. J. Med. Chem. 53, 283–291.

Zhang, M.Z., Chen, Q., Xie, C.H., Mulholland, N., Turner, S., Irwin, D., Gu, Y.C., Yang, G. F., Clough, J., 2015. Synthesis and antifungal activity of novel streptochlorin analogues. Eur. J. Med. Chem. 92, 776–783.

Zhang, A.W., Song, R.J., Wang, R.H., Li, H.D., Hu, D.Y., Song, B.A., 2022. Synthesis and antibacterial activities of 2-oxo-N-phenylacetamide derivatives containing a dissulfone moiety target on Clp. J. Agric. Food Chem. 70, 9356–9366.

Zhang, J.H., Wei, C.L., Li, S.Y., Hu, D.Y., Song, B.A., 2020. Discovery of novel bis-sulfoxide derivatives bearing acylhydrazone and benzothiazole moieties as potential antibacterial agents. Pestic. Biochem. Phys. 167, 104605.

Zhang, C., Zhou, T., Zhu, L., Juhasz, A., Du, Z., Li, B., Wang, J., Wang, J., Sun, Y., 2019. Response of soil microbes after direct contact with pyraclostrobin in fluvo-aquic soil. Environ. Pollut. 255, 113164.

Zhou, Y., Cai, M., Zhou, H., Hou, L.F., Peng, H., He, H.W., 2021. Discovery of efficient inhibitors against pyruvate dehydrogenase complex component E1 with bactericidal activity using computer aided design. Pestic. Biochem. Phys. 177, 104894.

Zhu, F.D., Fu, X., Ye, H.C., Ding, H.X., Gu, L.S., Zhang, J., Guo, Y.X., Feng, G., 2023. Antibacterial activities of coumarin-3-carboxylic acid against Acidovorax citrulli. Front. Microbiol. 14, 1207125.